Multipartite nonlocality in one-dimensional quantum spin chains at finite temperatures

Zhao-Yu Sun,[1,*] Meng Li [ORCID],[1] Long-Hui Sheng,[2] and Bin Guo[2]

[1]*School of Electrical and Electronic Engineering, Wuhan Polytechnic University, Wuhan 430023, China*
[2]*Department of Physics, Wuhan University of Technology, Wuhan 430070, China*

Multipartite nonlocality is an important measure of multipartite quantum correlations. In this paper, we show that the nonlocal n-site Mermin-Klyshko operator $\hat{M}_n$ can be exactly expressed as a matrix product operator with a bond dimension $D = 2$, and then the calculation of nonlocality measure $\mathcal{S}$ can be simplified into standard one-dimensional (1D) tensor networks. With the help of this technique, we analyze finite-temperature multipartite nonlocality in several typical 1D spin chains, including an XX model, an XXZ model, and a Kitaev model. For the XX model and the XXZ model, in a finite-temperature region, the logarithm measure of nonlocality ($\log_2 \mathcal{S}$) is a linear function of the temperature T, i.e., $\log_2 \mathcal{S} \sim -aT + b$. It provides us with an intuitive picture about how thermodynamic fluctuations destroy multipartite nonlocality in 1D quantum chains. Moreover, in the XX model $\mathcal{S}$ presents a magnetic-field-induced oscillation at low temperatures. This behavior has a nonlocal nature and cannot be captured by local properties such as the magnetization. Finally, for the Kitaev model, we find that in the limit $T \to 0$ and $N \to \infty$ the nonlocality measure may be used as an alternative order parameter for the topological-type quantum phase transition in the model.

I. INTRODUCTION

Quantum entanglement is a well-known concept in the fields of quantum information and condensed-matter physics [1–5]. For instance, as bipartite measures of entanglement, entanglement concurrence [6] and entanglement entropy [7] have been widely used to characterize quantum phase transitions (QPTs) [8] in various quantum systems. It needs mention that, in addition to *bipartite* entanglement, it is also quite natural to consider *multipartite* correlations in quantum many-body systems [9,10]. A feasible method to analyze multipartite correlations is to use Bell-type inequalities [11–20]. In the literature, multipartite correlation observed by Bell-type inequalities is usually called multipartite nonlocality.

Despite the complexity involved in its definition and calculations, multipartite nonlocality has still been used to study various low-dimensional spin lattices, including one-dimensional (1D) spin chains [21–27], spin ladders [28], two-dimensional (2D) quantum lattices [29], and the Lipkin-Meshkov-Glick model [30]. Some interesting behaviors have been reported. For instance, careful analysis of the ground-state nonlocality discloses that QPTs are usually accompanied by dramatic changes of the *hierarchy* of multipartite correlations [24]. Moreover, nonlocality also deepens our understanding about boundary effects in spin chains [31]. One can see that multipartite nonlocality indeed offers us a valuable perspective to characterize low-dimensional quantum models.

Previous studies about multipartite nonlocality in low-dimensional quantum systems are mainly about zero temperature. In this paper, we will extend the studies to finite

temperatures. Our first motivation is that, according to the third law of thermodynamics, real materials are inevitably affected by thermal fluctuations. We would like to mention that thermal-state nonlocality has been studied in several models [21,30]. Limited by their algorithms, nevertheless, only small lattices with $N \leqslant 12$ have been studied. Thereby, the picture about finite-temperature nonlocality in low-dimensional quantum models is far from complete.

The second motivation to consider finite temperatures is that in some quantum systems the ground states are (highly) degenerate, for instance, in some quantum models with long-range topological order [32,33]. As a result, when one uses some variational algorithms to figure out a ground state, the converged wave function may be any random state in the ground-state manifold. An alternative solution to overcome this randomness is to study the thermal-state density matrix $\hat{\rho}_T = e^{-\beta \hat{H}}$ with β the inversed temperature and $\hat{H}$ the Hamiltonian of the systems. It is clear that in the low-temperature limit $T \to 0$, $\hat{\rho}_T$ can capture *all* the bases of the ground-state manifold with equal weights. Thereby, it would be interesting to check whether the thermal-state nonlocality can be used to characterize these models.

In this paper, we will propose a tensor-network algorithm to calculate finite-temperature nonlocality in general quantum chains. Especially, we will show that a widely used nonlocality operator—the Mermin-Klyshko operator [34–36]—can be exactly rewritten as a matrix product operator (MPO) with a bond dimension $D = 2$. Then the calculation of nonlocality can be simplified into standard 1D tensor networks [37]. We will use the algorithm to study finite-temperature nonlocality in several typical 1D quantum spin chains. We will report a quantitative formula which describes how thermodynamic fluctuations destroy multipartite nonlocality in the XX model and the XXZ model. Then in the Kitaev chain, we will show

---

*Corresponding author: sunzhaoyu2020@whpu.edu.cn

that the nonlocality measure can be used to characterize the topological-type QPT in the model.

This paper is organized as follows. In Sec. II, the concepts of Bell-type inequalities, multipartite nonlocality, and corresponding numerical algorithms will be introduced. In Sec. III, results for the XX model, the XXZ model, and the Kitaev chain will be reported. A summary will be given in Sec. IV, where some in-depth discussions about the MPO form of the Bell operators will also be presented.

II. MULTIPARTITE NONLOCALITY AND ALGORITHMS

In this section, first, we will introduce the concepts of Bell-type inequalities and multipartite nonlocality in Sec. II A. Previous algorithms for calculating nonlocality will be reviewed briefly in Sec. II B. The shortcoming of the algorithms will also be pointed out. To overcome this shortcoming, in Sec. II C we show how to rewrite the Mermin-Klyshko operator as an MPO with a bond dimension $D = 2$. Finally, we will propose a concise tensor network to calculate finite-temperature nonlocality in Sec. II D.

A. Bell-type inequalities and multipartite nonlocality

We will consider a quantum system consisting of n qubits. First, on each qubit i, one should define two observables as

$$\hat{m}_i = \boldsymbol{a}_i \cdot \boldsymbol{\sigma},$$
$$\hat{m}_i' = \boldsymbol{b}_i \cdot \boldsymbol{\sigma}, \qquad (1)$$

where $\boldsymbol{a}_i$ and $\boldsymbol{b}_i$ are unit vectors, and $\boldsymbol{\sigma} = [\hat{\sigma}_x, \hat{\sigma}_y, \hat{\sigma}_z]$. For convenience, we shall use a $2 \times 2 \times 2$ tensor $m_i(k_i)$ to denote these two observables, i.e., $m_i(0) = \hat{m}_i$ and $m_i(1) = \hat{m}_i'$. Then a general n-qubit full-correlation Bell operator is defined as [34–36,38]

$$\hat{M}_g(\underline{\boldsymbol{a}}) = \sum_{\mathbf{k} \in \{0,1\}^n} \beta_{k_1 k_2 \ldots k_n} m_1(k_1) m_2(k_2) \cdots m_n(k_n), \qquad (2)$$

where $\underline{\boldsymbol{a}}$ denotes a set of the $2n$ unit vectors, i.e., $\underline{\boldsymbol{a}} = \{\boldsymbol{a}_1, \boldsymbol{b}_1 \ldots \boldsymbol{a}_n, \boldsymbol{b}_n\}$, and $\mathbf{k}$ is a shorthand notion for $k_1 k_2 \cdots k_n$. The coefficient $\beta_{k_1 k_2 \ldots k_n}$ is arbitrary and should satisfy

$$\max_{\underline{\boldsymbol{a}}} \langle \hat{M}_g(\underline{\boldsymbol{a}}) \rangle \leqslant 1 \qquad (3)$$

for all product states. For some system (or some state), if the inequality is violated, one can conclude that the system contains some kind of quantum correlations, which is usually called *multipartite quantum nonlocality*.

It is quite clear that one can define different Bell operators by setting the coefficient $\beta_{k_1 k_2 \ldots k_n}$. In this paper, we will consider a special class of Bell operators proposed by Mermin, Klyshko, and Svetlichny (see Refs. [34–36]):

$$\hat{M}_{[1 \ldots n]} = \frac{1}{2} \hat{M}_{[1 \ldots n-1]} \otimes (\hat{m}_n + \hat{m}_n') \\ + \frac{1}{2} \hat{M}_{[1 \ldots n-1]}' \otimes (\hat{m}_n - \hat{m}_n'). \qquad (4)$$

It is usually called the Mermin-Klyshko operator (or Mermin-Svetlichny operator). In the formula, the operator $\hat{M}'$ is obtained by exchanging all the $\boldsymbol{a}_i$ and $\boldsymbol{b}_i$ in the corresponding operator $\hat{M}$. In this paper, we will use the symbol $\hat{M}_g$ to denote the general Bell operator, and $\hat{M}$ to denote the Mermin-Klyshko operator. It is not difficult to prove that the
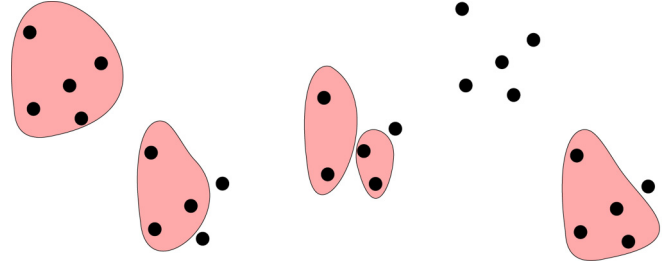
FIG. 1. Schematic diagram of various hierarchies of multipartite correlations. Pink shadow denotes that sites can share correlations only with others in the same group. Bell-type inequalities and the nonlocality measure $\mathcal{S}$ can capture the hierarchies of multipartite correlations in quantum states.

Mermin-Klyshko operator $\hat{M}$ is a special form of the general Bell operator $\hat{M}_g$. A key advantage of the Mermin-Klyshko operator is that it has explicit upper bounds for various hierarchies of multipartite nonlocality in many-body quantum systems [11,13–15], and thus can offer an intuitive description of multipartite quantum correlations in low-dimensional quantum lattices.

Hierarchy of multipartite nonlocality

Quantum systems which consist of many qubits can present various hierarchies of multipartite nonlocality. Please see Fig. 1. For a quantum state, in order to identify its hierarchy of multipartite nonlocality, one should consider the following high-rank Mermin-Klyshko inequalities [11,13–15]:

$$\mathcal{S} = \begin{cases} \max_{\underline{\boldsymbol{a}}} \langle \hat{M}_{[1 \ldots n]}(\underline{\boldsymbol{a}}) \rangle \leqslant 2^{\frac{n-g}{2}} & \text{for } n - g \text{ is even,} \\ \max_{\underline{\boldsymbol{a}}} \langle \hat{S}_{[1 \ldots n]}(\underline{\boldsymbol{a}}) \rangle \leqslant 2^{\frac{n-g}{2}} & \text{for } n - g \text{ is odd,} \end{cases} \qquad (5)$$

where the operator $\hat{S}_{[1 \ldots n]}$ is defined as

$$\hat{S}_{[1 \ldots n]} = \frac{1}{\sqrt{2}} \left(\hat{M}_{[1 \ldots n]} + \hat{M}_{[1 \ldots n]}' \right). \qquad (6)$$

$g = 2, 3, \ldots, n$ labels a full series of Mermin-Klyshko inequalities. In these inequalities, the highest-rank one is $\mathcal{S} \leqslant 2^{\frac{n-2}{2}}$. If it is violated, we can conclude that the quantum state contains the highest hierarchy of multipartite nonlocality, i.e., genuine multipartite nonlocality. The lowest-rank inequality is just $\mathcal{S} \leqslant 2^{\frac{n-n}{2}} = 1$. If $\mathcal{S} \leqslant 1$ is violated, we say that the state contains the lowest hierarchy of multipartite nonlocality.

In condensed-matter physics, we are just interested in the qualitative behavior of multipartite correlations, rather than the specific "hierarchy number." Thereby, we will ignore the parity in Eq. (5), and just consider the nonlocality measure $\mathcal{S} = \max_{\underline{\boldsymbol{a}}} \langle \hat{M}_{[1 \ldots n]}(\underline{\boldsymbol{a}}) \rangle$. Generally speaking, a *larger* value of $\mathcal{S}$ indicates that the quantum system presents a *higher* hierarchy of multipartite nonlocality.

B. Ground-state nonlocality

We will review previous algorithms to calculate nonlocality for 1D quantum chains at zero temperature [26]. The shortcoming of the algorithms will also be pointed out.

The entire procedure contains two steps. In step 1, one shall use matrix product states (MPS) to approximately describe

the ground states $|\psi\rangle$ of the concerned quantum chains [37]. In step 2, one needs to carry out a numerical optimization to figure out the nonlocality measure:

$$\mathcal{S} = \max_{\underline{a}} \langle\psi|\hat{M}_{[1...n]}(\underline{a})|\psi\rangle. \tag{7}$$

Multivariate optimization is a highly nontrivial problem, and a two-site update algorithm has been proposed to carry out the optimization [26]. The basic idea is to transform the n-site optimization into a series of two-site optimizations, and sweep the chains several times until some convergence is achieved. More technique details can be found in Ref. [26].

The objective function $\langle\psi|\hat{M}|\psi\rangle$ plays a central role in the optimization. In Ref. [26], in order to carry out the two-site update optimization, we have to decompose $\langle\psi|\hat{M}|\psi\rangle$ into the following four terms as $\langle\psi|\hat{M}|\psi\rangle = (f_1 + f_2 + f_3 - f_4) \times \frac{1}{2}$:

$$f_1 = \langle\psi|\hat{M}_{[1...k-1]} \otimes \hat{M}_{[k,k+1]} \otimes \hat{M}'_{[k+2...N]}|\psi\rangle,$$
$$f_2 = \langle\psi|\hat{M}'_{[1...k-1]} \otimes \hat{M}_{[k,k+1]} \otimes \hat{M}_{[k+2...N]}|\psi\rangle,$$
$$f_3 = \langle\psi|\hat{M}_{[1...k-1]} \otimes \hat{M}'_{[k,k+1]} \otimes \hat{M}_{[k+2...N]}|\psi\rangle,$$
$$f_4 = \langle\psi|\hat{M}'_{[1...k-1]} \otimes \hat{M}'_{[k,k+1]} \otimes \hat{M}'_{[k+2...N]}|\psi\rangle. \tag{8}$$

Moreover, in the above expressions, $\hat{M}_{[1...k-1]}$, $\hat{M}'_{[1...k-1]}$, $\hat{M}_{[k+2...N]}$, and $\hat{M}'_{[k+2...N]}$ also need to be treated carefully.

The shortcoming of the above algorithm is that the expression for the objective function $\langle\psi|\hat{M}|\psi\rangle$ is rather complex.

For a given MPS $|\psi\rangle$, it is well known that if an operator $\hat{O}$ can be expressed as an MPO its average value $\langle\psi|\hat{O}|\psi\rangle$ can be calculated conveniently [39]. The first contribution of this paper is that we will show the Mermin-Klyshko operator $\hat{M}_{[1...N]}$ can be expressed exactly as an MPO with a quite small bond dimension, i.e., $D = 2$.

C. Bell operators in the form of matrix product operators

First, we shall show that the general Bell operator $\hat{M}_g$ in Eq. (2) can be expressed as an MPO. For such a purpose, we will just consider an n-qubit 1D quantum chain which is in its ground state, i.e.,

$$|\psi\rangle = \sum_{\mathbf{s}' \in \{0,1\}^n} \alpha_{s'_1 s'_2...s'_n} |s'_1\rangle \otimes |s'_2\rangle \otimes \cdots |s'_n\rangle, \tag{9}$$

where $\mathbf{s}'$ is a shorthand notion for $s'_1 s'_2 \cdots s'_n$. It is well known that the coefficient tensor $\alpha_{s'_1 s'_2...s'_n}$ can be expressed efficiently as an MPS:

$$\alpha_{s'_1 s'_2...s'_n} = A_1(s'_1)A_2(s'_2) \cdots A_n(s'_n). \tag{10}$$

Similarly, for the general Bell operator $\hat{M}_g$ in Eq. (2), we can treat its coefficient $\beta_{k_1 k_2...k_n}$ as a high-rank tensor. Through a series of singular value decompositions (SVDs), $\beta_{k_1 k_2...k_n}$ can also be decomposed into an MPS, i.e.,

$$\beta_{k_1 k_2...k_n} = B_1(k_1)B_2(k_2) \cdots B_n(k_n). \tag{11}$$

We are ready to consider the expectation value $\langle\psi|\hat{M}_g|\psi\rangle$. According to Eqs. (2), (9), (10), and (11), it is straightforward
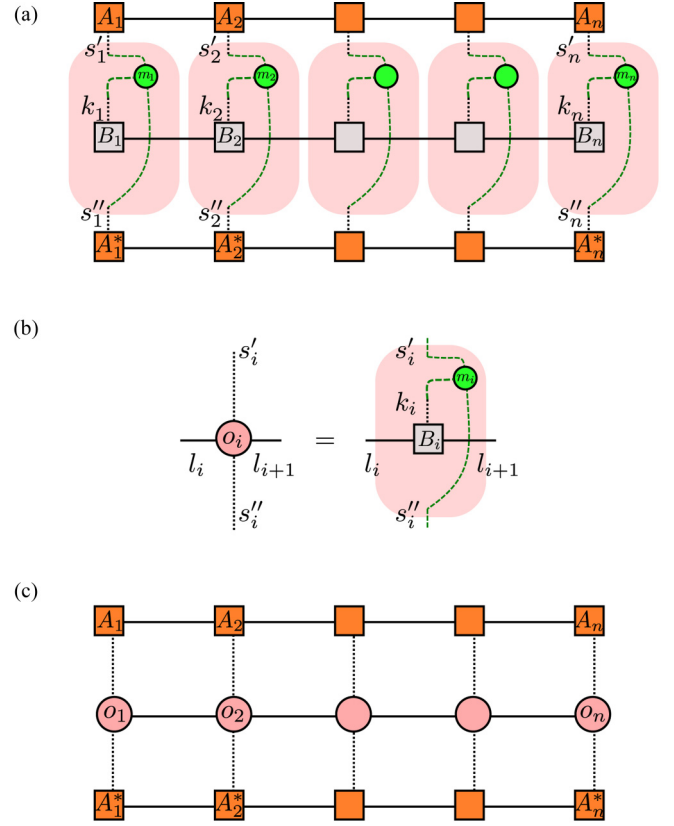
FIG. 2. (a) Tensor network illustrating the expectation value $\langle\psi|\hat{M}_g|\psi\rangle$ for the general full-correlation Bell operator [Eq. (12)]. The ground-state wave function $|\psi\rangle$ is in the form of a matrix product state (see the orange squares). By defining local tensors o_i in (b), the tensor network in (a) is further rephrased into a standard 1D three-layer tensor network, where the Bell operator is in the form of a matrix product operator with bond dimensions up to $2^{\frac{n}{2}}$.

that $\langle\psi|\hat{M}_g|\psi\rangle$ can be rephrased as

$$\langle\psi|\hat{M}_g|\psi\rangle = \sum_{\mathbf{s}'} \sum_{\mathbf{k}} \sum_{\mathbf{s}''} \alpha_{\mathbf{s}'} \beta_{\mathbf{k}} \alpha^*_{\mathbf{s}''} \langle s'_1|m_1(k_1)|s''_1\rangle$$
$$\times \langle s'_2|m_2(k_2)|s''_2\rangle \cdots \langle s'_n|m_n(k_n)|s''_n\rangle. \tag{12}$$

In Fig. 2(a) we have drawn a tensor network to illustrate the above expression, where $\alpha_{\mathbf{s}'}$, $\beta_{\mathbf{k}}$, and $\alpha^*_{\mathbf{s}''}$ have been described as standard 1D tensor networks, and the expression $\langle s'_1|m_1(k_1)|s''_1\rangle\langle s'_2|m_2(k_2)|s''_2\rangle \cdots \langle s'_n|m_n(k_n)|s''_n\rangle$ is denoted by a direct product of local tensors. Thereby, the expectation value $\langle\psi|\hat{M}_g|\psi\rangle$ is completely decomposed into contractions of local tensors.

To proceed, on each qubit i, we shall further define a tensor $o_i = m_i B_i$ [see Fig. 2(b)]. Then $\langle\psi|\hat{M}_g|\psi\rangle$ is further rephrased as a concise 1D tensor network in Fig. 2(c), that is,

$$\hat{M}_g = \langle o_1|\hat{o}_2\hat{o}_3\hat{o}_4...|o_n\rangle. \tag{13}$$

In the language of tensor networks [37,39,40], the right-hand side of Eq. (13) is a standard MPO. It needs mention that, generally speaking, the obtained MPO should have a bond dimension as large as $D = 2^{\frac{n}{2}}$. Some advanced compression techniques may be used to compress this MPO [39,41,42].

Now we consider the Mermin-Klyshko operator. Thanks to its recursive definition in Eq. (4), we do not need to first figure out the coefficient tensor $\beta_{k_1 k_2 ... k_n}$ and then carry out the SVD decompositions. Instead, the recursive expression in Eq. (4) reminds us about how 1D quantum chains are treated with the famous infinite-size density-matrix renormalization-group algorithm [37,39,40], where the Hamiltonian can be expressed concisely as an MPO with a quite small bond dimension.

Along a similar procedure, we have successfully figured out an MPO expression for the Mermin-Klyshko operator, with a bond dimension $D = 2$. The derivation process just follows Refs. [39,40], and we shall just provide the final result in this paper. Let us consider an n-site chain. For the leftmost site, based upon the single-site operators $\hat{m}_k$ and $\hat{m}'_k$ defined in Eq. (1), let us define a *bra* as

$$\langle o_1| = (\hat{m}_1, \hat{m}'_1). \tag{14}$$

For the rightmost site, we define a *ket* as

$$|o_n\rangle = \begin{pmatrix} \frac{1}{2}(\hat{m}_n + \hat{m}'_n) \\ \frac{1}{2}(\hat{m}_n - \hat{m}'_n) \end{pmatrix}. \tag{15}$$

For each intermediate site $1 < i < n$, we further define a 2×2 operator-valued matrix as

$$\hat{o}_i = \begin{pmatrix} \frac{1}{2}(\hat{m}_i + \hat{m}'_i) & \frac{1}{2}(\hat{m}'_i - \hat{m}_i) \\ \frac{1}{2}(\hat{m}_i - \hat{m}'_i) & \frac{1}{2}(\hat{m}_i + \hat{m}'_i) \end{pmatrix}. \tag{16}$$

Then one can check that the Mermin-Klyshko operator is equal to the product of these local tensors:[1]

$$\hat{M}_{[1...n]} = \langle o_1|\hat{o}_2\hat{o}_3\hat{o}_4...|o_n\rangle, \tag{17}$$

i.e., an MPO. According to Eqs. (14)–(16), the bond dimension of this MPO is merely $D = 2$.

Alternatively, one can check that the Mermin-Klyshko operator can be expressed as a general full-correlation Bell operator, where its coefficient $\beta_{k_1 k_2 ... k_n}$ has a concise MPS form in Eq. (11), with $B_i(k_i)$ given by

$$\begin{aligned} B_1(0) &= (1, 0), & B_1(1) &= (0, 1), & i &= 1; \\ B_i(0) &= \begin{pmatrix} \frac{1}{2} & -\frac{1}{2} \\ \frac{1}{2} & \frac{1}{2} \end{pmatrix}, & B_i(1) &= \begin{pmatrix} \frac{1}{2} & \frac{1}{2} \\ -\frac{1}{2} & \frac{1}{2} \end{pmatrix}, & 1 &< i < n; \\ B_n(0) &= \begin{pmatrix} \frac{1}{2} \\ \frac{1}{2} \end{pmatrix}, & B_n(1) &= \begin{pmatrix} \frac{1}{2} \\ -\frac{1}{2} \end{pmatrix}, & i &= n. \end{aligned} \tag{18}$$

Finally, with the help of Eq. (17), the objective function $\langle\psi|\hat{M}|\psi\rangle$ can be expressed concisely as a standard 1D tensor network. Please see Fig. 3(a). Various mature software, such as ITENSOR [43], can contract this network conveniently.

D. Finite-temperature nonlocality

We move on to show how to calculate nonlocality in a spin chain at finite temperatures. The quantum state of the system

---

[1]The operator $\hat{S}_{[1...n]}$ in Eq. (6) can also be expressed as a matrix product operator. On the rightmost site let us define a *ket* as $|\tilde{o}_n\rangle = \frac{1}{\sqrt{2}}\begin{pmatrix}\hat{m}'_n\\\hat{m}_n\end{pmatrix}$, then it is not difficult to prove that $\hat{S}_{[1...n]} = \langle o_1|\hat{o}_2\hat{o}_3\hat{o}_4 ... |\tilde{o}_n\rangle$.
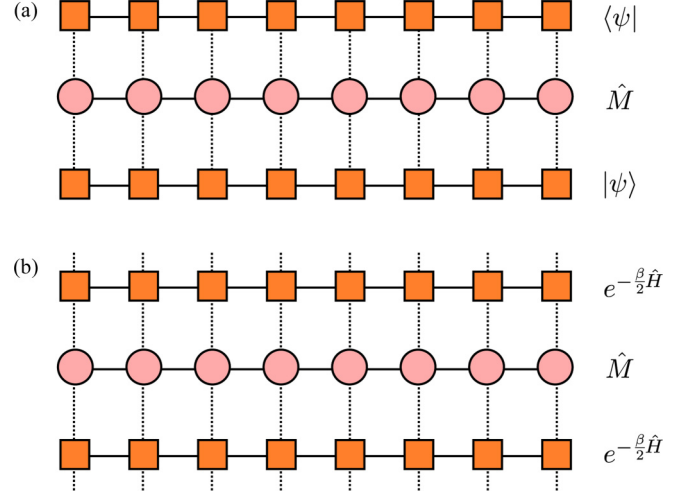
FIG. 3. (a) Tensor network illustrating the ground-state expectation value $\langle\psi|\hat{M}|\psi\rangle$ for the Mermin-Klyshko operator. The ground state $|\psi\rangle$ is in the form of a matrix product state (see the origin squares). The Mermin-Klyshko operator $\hat{M}$ is in the form of a matrix product operator with a bond dimension $D = 2$ (see the circles). (b) Tensor network used in calculating finite-temperature nonlocality. The thermal-state operator $e^{-\beta\hat{H}}$ is expressed in a quadratic form to maintain its positive definiteness, and periodic boundary conditions should be imposed in the vertical direction. These standard 1D tensor networks can be contracted conveniently by mature software, such as ITENSOR [43].

shall be described by a thermal-state operator $e^{-\beta\hat{H}}$, where $\hat{H}$ is the Hamiltonian of the quantum chain, and $\beta = \frac{1}{k_B T}$ is the inversed temperature. The Boltzmann constant is set as $k_B = 1$.

First of all, one shall figure out $e^{-\beta\hat{H}}$. For such a purpose, we will use the standard imaginary-time-evolution algorithm [41]. The basic idea is as follows. We start from an imaginary-time-evolution operator:

$$\hat{U}_1 = e^{-\Delta\tau\hat{H}}, \tag{19}$$

where $\Delta\tau$ is a small number (for instance, $\Delta\tau = 0.05$) denoting a time slice. $\hat{U}_1$ can be expressed as an MPO faithfully by a second-order Trotter-Suzuki approximation [41]. Then we carry out the following recursive procedure:

$$\hat{U}_m = \hat{U}_{m-1}\hat{U}_1. \tag{20}$$

It is clear that at the mth step the operator $\hat{U}_m$ is equal to $e^{-\beta_m\hat{H}}$ with $\beta_m = m\Delta\tau$. Thereby, as the recursive procedure continues, the temperature $T = \frac{1}{\beta_m} = \frac{1}{m\Delta\tau}$ gradually decreases.

In practice, the bond dimension of the matrix product operator $\hat{U}_m$ would increase *exponentially* as m increases. Thereby, we would use some mature compression method [39,41] to keep the bond dimension of $\hat{U}_m$ controllable. Moreover, in order to maintain the positive definiteness of the thermal-state operator $e^{-\beta\hat{H}}$, it is helpful to use the square of $\hat{U}_m$ to construct $e^{-\beta\hat{H}}$, i.e., $\hat{U}_m\hat{U}_m \rightarrow e^{-\beta\hat{H}}$ [41]. Thus, at step m, the actual temperature becomes $T = \frac{1}{2m\Delta\tau}$. Finally, we should normalize the thermal state as $\frac{e^{-\beta\hat{H}}}{\text{Tr}e^{-\beta\hat{H}}}$.

(a) subchain nonlocality $\mathcal{S}(\hat{\rho}_{\mathrm{subchain}})$

$\hat{\rho}_{\mathrm{subchain}}$

(b) global nonlocality $\mathcal{S}(\hat{\rho}_T)$

$\hat{\rho}_T$
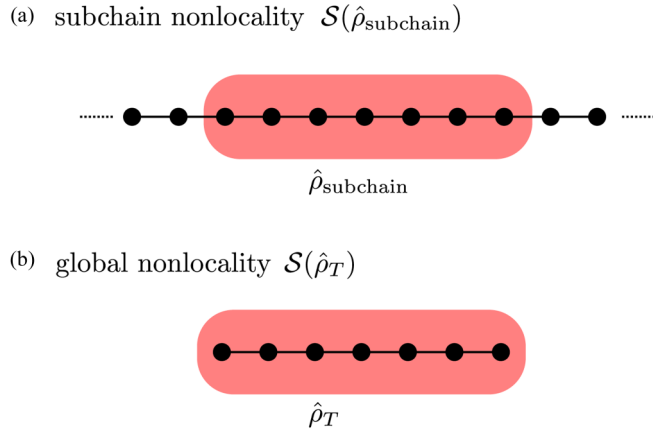
FIG. 4. Two approaches are used in this paper to investigate nonlocality in quantum chains. (a) Subchain nonlocality is defined on the reduced density matrices of continuous n-site subchains in infinite-size chains. (b) Global nonlocality is defined on the density matrices of entire finite-size chains with total length N.

After figuring out the normalized thermal state $e^{-\beta\hat{H}}$, we are ready to calculate the nonlocality measure:

$$\mathcal{S} = \max_{\underline{a}} \mathrm{Tr}\big[\hat{M}_{[1...N]}(\underline{a}) \cdot e^{-\beta\hat{H}}\big]. \tag{21}$$

It is straightforward that the objective function can be expressed as a 1D tensor network as shown in Fig. 3(b). The optimization should follow the idea of the two-site update algorithm in Ref. [26].

III. MODELS AND MAIN RESULTS

In this paper, we will consider three typical 1D quantum chains (i.e., the XX model, the XXZ model, and the Kitaev chain) at finite temperatures. A direct calculation of the nonlocality for the entire infinite-size chains is intractable. Thereby, we will investigate "subchain nonlocality" [Fig. 4(a)] by considering continuous n-site subchains in infinite-size systems. When necessary, we will also investigate "global nonlocality" [Fig. 4(b)] in the entire finite-size chains with total length N.

Some numerical details are as follows. In calculating the thermal-state operator $e^{-\beta\hat{H}}$, $\Delta\tau$ is set to 0.05, and a second-order Trotter-Suzuki decomposition is used. The maximum bond dimension for the matrix product operator $\hat{U}_m$ is $D_0 = 40$–80. In the numerical optimization of Eq. (21), in order to obtain reliable results, for each set of physical parameters, we use 20 independent initial points to carry out the optimizations.

A. XX model

The 1D antiferromagnetic XX model under a magnetic field is described by [45,46]

$$\hat{H} = \sum_i \big(\hat{\sigma}_x^i \hat{\sigma}_x^{i+1} + \hat{\sigma}_y^i \hat{\sigma}_y^{i+1}\big) - h \sum_i \hat{\sigma}_z^i. \tag{22}$$

$\hat{\sigma}_{x,y,z}^i$ denote Pauli matrices on site i. The first summation denotes the nearest-neighboring interaction in the x-y plane. h denotes the strength of the magnetic field along the z direction.
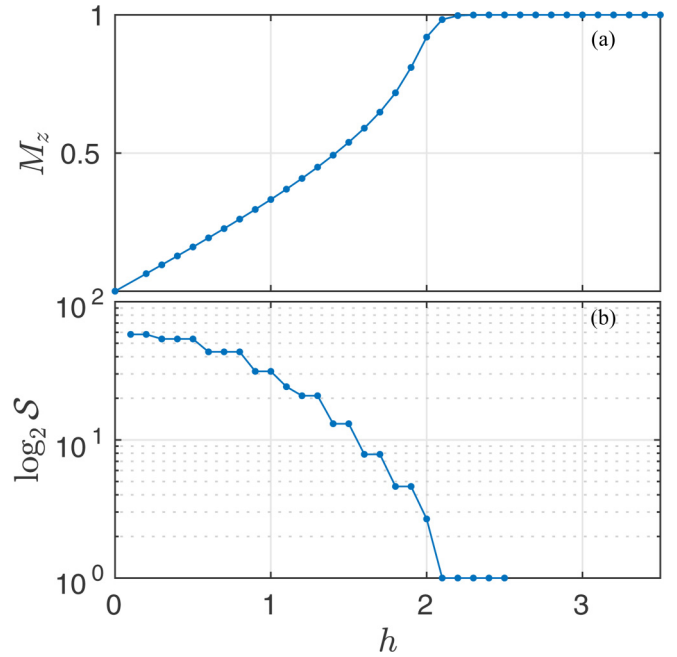
FIG. 5. (a) Magnetization curve of the infinite-size XX model at a finite temperature $T = 0.1$. h denotes the magnetic field, and $h_c = 2$ is the ground-state QPT point. (b) Influence of the magnetic field upon the global nonlocality in the entire XX chain by considering a finite-size model with $N = 20$ and $T = 0$. The ground state is calculated by ALPS [44] with a maximum bond dimension $D = 100$.

$h_c = 2$ is the ground-state QPT point of the model. Figure 5(a) shows the magnetization curve of the model at a fixed temperature $T = 0.1$. Figure 5(b) offers a brief description about the effect of the magnetic field upon the global nonlocality by considering a finite-size chain. It is clear that the magnetic field tends to destroy the global nonlocality in the model.

Then we pay our attention to subchain nonlocality. First of all, in Fig. 6(a), we have shown the subchain nonlocality as a function of the magnetic field in the infinite-size XX model at finite temperatures. One can find that in the two phases $h < h_c$ and $h > h_c$, the nonlocality measure $\mathcal{S}$ presents quite different behavior. We take the curve with $T = 0.1$ for instance. For $h > h_c$, it holds that $\mathcal{S} \leqslant 1$, thus the Mermin-Klyshko inequality in Eq. (5) is not violated and nonlocality is not observed. For most areas in $h < h_c$, nevertheless, $\mathcal{S}$ is larger than 1, thus nonlocality is observed. In fact, in Fig. 6(a), in some regions the value of $\mathcal{S}$ is larger than 8. According to Eq. (5), some high hierarchy of multipartite nonlocality is observed.

Furthermore, in the phase $h < h_c$, it is remarkable that the $\mathcal{S}(h)$ curve presents a clear oscillation behavior. As the temperature increases, the amplitude of the oscillation is suppressed gradually. However, one sees that the oscillation can still be observed with the temperature up to $T = 0.5$. Finally, when the temperature is high enough (i.e., $T = 1$), the nonlocality measure $\mathcal{S}$ vanishes.

The oscillation of the nonlocality discloses that, behind the simple magnetization curve in Fig. 5(a), there is a hidden and rich change of multipartite correlations in the reduced density matrices $\hat{\rho}_n$ of the subchains. Real materials always contain countless atoms. In real experiments, nevertheless, due to the
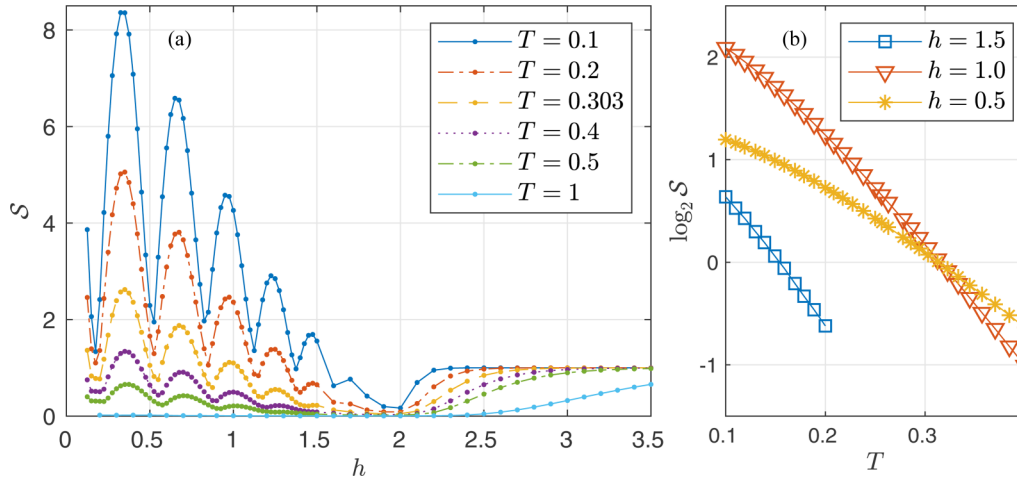
FIG. 6. (a) Subchain-nonlocality measure $\mathcal{S}$ as a function of the magnetic field h in the infinite-size XX model at finite temperatures T. The length of the subchain is $n = 20$. It is remarkable that in the phase $h < h_c = 2$, $\mathcal{S}$ presents a magnetic-field-induced oscillation at low temperatures. This rich behavior in multipartite nonlocality cannot be captured by studying local properties such as the magnetization (see Fig. 5). (b) Logarithm measure $\log_2 \mathcal{S}$ as a function of T with several h. In a finite-temperature region, $\log_2 \mathcal{S}$ presents an approximate linear decrement. It provides us with an intuitive picture about how the nonlocality gradually disappears as the temperature rises.

actual size of the equipment, only a limited number of atoms would be measured. Thereby, an oscillation curve of subchain nonlocality [Fig. 6(b)], rather than the monotonic decreasing curve of the global nonlocality [Fig. 5(b)], is more likely to be observed in an experiment.

We would like to mention that the oscillation behavior of nonlocality has also been reported in a zero-temperature spin ladder in a quite recent paper [28]. In Ref. [28], by using careful numerical analysis, the authors have pointed out that the mechanism for the oscillation of the nonlocality is the "major component transitions" in the reduced density matrices $\hat{\rho}_n$ of the subchains. Moreover, they have found that the oscillation of the subchain nonlocality would be modulated by global nonlocality. Comparing Figs. 5(b) and 6(a), one sees that the envelope curve of the subchain-nonlocality oscillation in Fig. 6(a) is a monotonic decreasing curve, which is indeed quite similar to the global-nonlocality curve in Fig. 5(b). Nevertheless, the results reported in this model have additional contributions. First, our results ambitiously indicate that the oscillation of the nonlocality can survive at finite temperatures, thus may be observed in laboratory. In addition, our results reveals how the oscillation is suppressed gradually as the temperature rises. Secondly, comparing the oscillation behavior in the XX model and in the ladder model [28], we find three common characteristics: Both models have $U(1)$ symmetry; oscillation occurs in the procedure where the models are being polarized by an external magnetic field; oscillation is observed in subchain nonlocality, but not in global nonlocality in the entire lattice. We hope these features point us in the right direction to search for similar phenomena.

Figure 6(a) also shows that as the temperature rises nonlocality weakens gradually. In order to draw a more intuitive picture about the effect of the temperature upon the nonlocality, in Fig. 6(b) we have illustrated the logarithm measure $\log_2 \mathcal{S}$ as a function of the temperature T. It needs mention that $\mathcal{S} = 1$ (i.e., $\log_2 \mathcal{S} = 0$) is the threshold value of the lowest-rank Mermin-Klyshko inequality $\mathcal{S} \leqslant 1$. One can see that (at least) in the vicinity of the threshold value $\log_2 \mathcal{S} = 0$,

the logarithm measure $\log_2 \mathcal{S}$ can be expressed as a linear function of T approximately, i.e.,

$$\log_2 \mathcal{S} \approx -aT + b. \tag{23}$$

It is well known that in the high-temperature limit $T \to \infty$ all correlations (including quantum nonlocality) should vanish. On the other hand, in the low-temperature region $T \approx 0$, the behavior of quantum nonlocality should be determined by the lowest-lying energy states. However, in the middle-temperature regions, a general description is still unclear. The linear behavior reported in Fig. 6(b) supplements part of the missing picture in the middle-temperature regions. As we will show in the next section, the behavior in Eq. (23) is also observed in the XXZ model.

B. XXZ model

The 1D XXZ model is described by the Hamiltonian [8,22]

$$\hat{H} = \sum_i \left(\hat{\sigma}_x^i \hat{\sigma}_x^{i+1} + \hat{\sigma}_y^i \hat{\sigma}_y^{i+1} + \Delta \hat{\sigma}_z^i \hat{\sigma}_z^{i+1} \right), \tag{24}$$

where Δ is the anisotropic parameter. The ground-state phase diagram of the model is quite clear [22]. In the limit $\Delta \to \infty$ and $\Delta \to -\infty$, the model would be in an antiferromagnetic state and a ferromagnetic state, respectively. It is expected that in the intermediate regions one or more QPTs should take place. Further research shows that there is a first-order QPT at $\Delta = -1$ and an infinite-order QPT at $\Delta = +1$.

The zero-temperature nonlocality of the XXZ model has been studied in several papers [22,25]. We will pay our attention to finite-temperature nonlocality in the model and concentrate on a positive Δ. In Fig. 7(a) we have shown the dependence of the subchain nonlocality upon the anisotropic parameter Δ at several temperatures. First of all, when the temperature is high enough (i.e., $T = 0.5$ and 1), the value of nonlocality measure $\mathcal{S}$ is quite small, thus the lowest-rank Mermin-Klyshko inequality $\mathcal{S} \leqslant 1$ is not violated at all. In other words, nonlocality is not present at high temperatures.
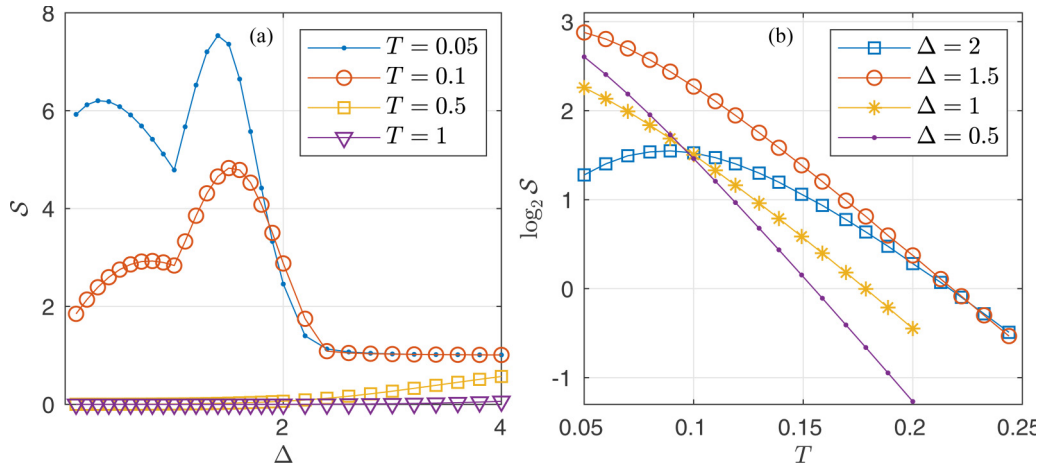
FIG. 7. (a) Subchain-nonlocality measure $\mathcal{S}$ as a function of the anisotropic parameter Δ in the infinite-size XXZ model at finite temperatures T. The length of the subchain is $n = 20$. It is remarkable that $\mathcal{S}$ presents cusplike singularity at the QPT point $\Delta_c = 1$ at finite temperatures. (b) Logarithm measure $\log_2 \mathcal{S}$ as a function of T with several Δ. Similar to Fig. 6 for the XX model, $\log_2 \mathcal{S}$ in the XXZ model also presents a linear decrement in a finite-temperature region. Moreover, when $\Delta = 2$, we observe some thermal enhancement of $\mathcal{S}$ in the low-temperature regions $T \leqslant 0.9$.

Then we turn our attention to low temperatures. Let us take $T = 0.05$ for instance. We find that the $\mathcal{S}(\Delta)_{T=0.05}$ curve is quite similar to the zero-temperature curve previously reported in Ref. [25]. First, in most regions, one can see that $\mathcal{S} > 1$, thus multipartite nonlocality is indeed observed. Second, at the QPT point $\Delta_c = 1$, $\mathcal{S}$ presents a cusplike singularity. When the temperature is enhanced from $T = 0.05$ to 0.1, this cusplike singularity survives, and the location is still at $\Delta_c = 1$. This result indicates that this QPT can be detected by multipartite nonlocality even at finite temperatures.

In Fig. 7(a), for most values of Δ, increasing temperature tends to destroy quantum nonlocality. However, in a narrow region near $\Delta = 2$, we observe a thermal enhancement behavior. That is, the $\mathcal{S}(\Delta)_{T=0.1}$ curve is above the $\mathcal{S}(\Delta)_{T=0.05}$ curve. This thermal enhancement should be due to the influence of low-lying excited states. We denote the ground state and the first excited state as $|\psi_0\rangle$ and $|\psi_1\rangle$, respectively. First of all, when the temperature T is low enough, the thermal state $e^{-\beta \hat{H}}$ can be approximately expressed as $e^{-\beta \hat{H}} \approx \omega_0 |\psi_0\rangle\langle\psi_0| + \omega_1 |\psi_1\rangle\langle\psi_1|$, with ω_i the weights of corresponding states. When $T = 0$, the system should be in the ground state, thus $\omega_0 = 1$ and $\omega_1 = 0$. As the temperature increases and is slightly larger than zero, the weight ω_0 for the ground state $|\psi_0\rangle$ decreases and the weight ω_1 for the first excited state $|\psi_1\rangle$ increases gradually. Suppose $|\psi_1\rangle$ contains more quantum nonlocality than $|\psi_0\rangle$; it is expected that there will be a thermal enhancement in the low-temperature regions. This is just what happens in the vicinity of $\Delta = 2$ in the XXZ model in Fig. 7.

In order to offer an intuitive picture about how the temperature affects the subchain nonlocality in the XXZ model, we have plotted the logarithm measure $\log_2 \mathcal{S}$ as a function of T in Fig. 7(b). First, when $\Delta = 2$, in the low-temperature regions one can see the thermal enhancement of $\mathcal{S}$ clearly. Second, just as in the XX model in the previous section, we find that (at least) in the vicinity of the threshold value $\log_2 \mathcal{S} = 0$, the logarithm measure $\log_2 \mathcal{S}$ can also be ex-

pressed as a linear function of T approximately, i.e., $\log_2 \mathcal{S} \approx -aT + b$.

C. Kitaev chain

We will consider a 1D Kitaev chain described by [32,47]

$$\hat{H} = J_1 \sum_{\text{even bonds}} \hat{\sigma}_x^i \hat{\sigma}_x^{i+1} + J_2 \sum_{\text{odd bonds}} \hat{\sigma}_y^i \hat{\sigma}_y^{i+1}, \quad (25)$$

where its structure is shown in Fig. 8. On even and odd bonds, spin-spin interactions only occur along the x and y directions, respectively. J_1 and J_2 are corresponding coupling constants. In fact, the Kitaev chain is just a 1D simplified version of the Kitaev model on a 2D honeycomb lattice introduced by Kitaev (see Refs. [47,48]).

For the Kitaev chain defined in Eq. (25), it is convenient to denote a coupling ratio as $\gamma = J_1/J_2$, and then the Hamiltonian is just controlled by γ. It has been found that the second derivative of the ground-state energy density diverges at $\gamma = 1$ [32]. Moreover, the energy gap between the ground states and other low-lying excited states also vanishes at $\gamma = 1$. Thus $\gamma_c = 1$ is indeed a QPT point. Further studies show that the string order parameter (denoted as Δ_x in Ref. [32]) is zero for $\gamma_c < 1$ and nonzero for $\gamma_c > 1$. Thereby, the phase transition is accompanied by a change of the topological order in the chain.
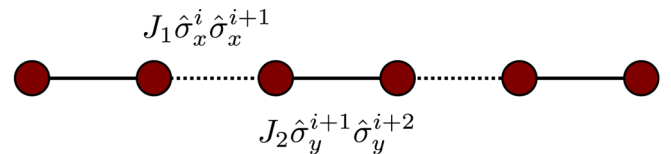
FIG. 8. Structure of Kitaev chains. J_1 and J_2 denote the coupling constants in the even bonds and odd bonds, respectively. We use $\gamma = J_1/J_2$ to denote the coupling ratio, and $\gamma_c = 1$ is the topological QPT point in the ground states of the model.
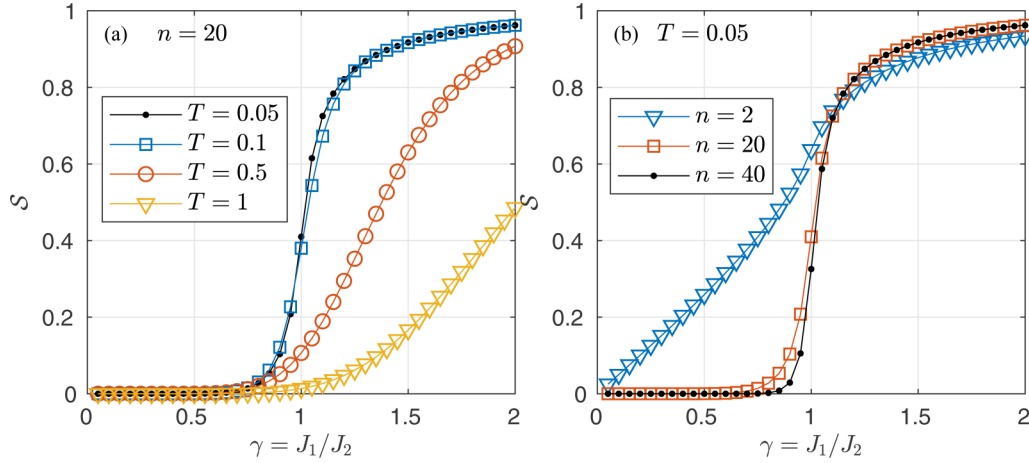
FIG. 9. (a) Subchain-nonlocality measure $\mathcal{S}$ as a function of the coupling ratio $\gamma = J_1/J_2$ in the infinite-size Kitaev chains at finite temperatures T. The length of the subchain is $n = 20$. $\gamma_c = 1$ is the ground-state topological QPT point. (b) The influence of the subchain length n upon the nonlocality curve $\mathcal{S}(\gamma)$. These results indicate that in the limit $T \to 0$ and $n \to \infty$, $\mathcal{S}$ can be used as an order parameter for the QPT of the Kitaev chains.

It needs mention that for any finite γ, the ground states of the Kitaev chain are always degenerate, labeled as $|\psi_1\rangle$, $|\psi_2\rangle$, and so on. As a result, when one uses some variational algorithms to figure out a ground state, the converged wave function may be any random state in the subspace spanned by $\{|\psi_i\rangle\}$. An alternative solution to overcome this randomness is to study the thermal state $\hat{\rho}_T$. In the low-temperature limit, the thermal state would become an equally weighted mixed state of these ground states, i.e., $\hat{\rho}_T \to \sum_j |\psi_j\rangle\langle\psi_j|$. As we will show, the nonlocality in this thermal state can be used to characterize the topological QPT in the Kitaev chain.

In Fig. 9(a) we have illustrated the subchain nonlocality as a function of the coupling ratio $\gamma = J_1/J_2$ with various T. When the temperature is low enough (i.e., $T = 0.05$ and 0.1), one can see that in most regions of $\gamma < 1$ the measure $\mathcal{S}$ is simply zero, while for $\gamma > 1$ $\mathcal{S}$ is nonzero. Furthermore, we pay our attention to the vicinity of $\gamma_c = 1$. When the temperature decreases from $T = 0.1$ to 0.05, in the regions $\gamma \lesssim 1$ and $\gamma \gtrsim 1$, the value of $\mathcal{S}$ becomes slightly smaller and bigger, respectively. It is a clue that in the limit $T \to 0$ the first-order derivative of the measure $\mathcal{S}$ would diverge at $\gamma_c = 1$.

In Fig. 9(b), we move on to investigate the effect of the length n of the subchains upon the nonlocality measure $\mathcal{S}$. When n is small, i.e., $n = 2$, we find that $\mathcal{S}$ is nonzero for any finite γ. When n increases to 20, $\mathcal{S}$ vanishes for most regions in $\gamma < 1$. When n increases from 20 to 40, in the vicinity of $\gamma_c = 1$, the value of $\mathcal{S}$ is further reduced. It is expected that in the limit $n \to \infty$ and $T \to 0$, the nonlocality measure $\mathcal{S}$ would be zero for $\gamma < \gamma_c$ and nonzero for $\gamma > \gamma_c$. In other words, just as the string order parameter proposed in Ref. [32], $\mathcal{S}$ may serve as an alternative order parameter for the QPT in the Kitaev chain.

In Fig. 9, for the subchain nonlocality measure $\mathcal{S}$, it holds that $\mathcal{S} \leqslant 1$ for any T and γ. In fact, as can be seen in Fig. 9(a), the $\mathcal{S}(\gamma)_{T=0.05}$ curve and the $\mathcal{S}(\gamma)_{T=0.1}$ curve almost overlap each other. Moreover, in Fig. 9(b), the $\mathcal{S}(\gamma)_{n=20}$ curve and the $\mathcal{S}(\gamma)_{n=40}$ curve also overlap with each other. It indicates that convergence has been achieved and one should still have

$\mathcal{S} \leqslant 1$ in the large-n and low-T limits. In other words, we do not expect to observe nonlocality in the subchains. In the XX model and XXZ model, nevertheless, we have identified some high hierarchy of multipartite nonlocality, indicated by the relatively large value of the nonlocality measure $\mathcal{S}$ in Figs. 6 and 7. Thereby, when multipartite correlations are concerned, the Kitaev chain is qualitatively different from the XX model and XXZ model.

We would like to mention that in some states, for instance, in the Greenberger-Horne-Zeilinger (GHZ) state $|GHZ\rangle = \frac{1}{\sqrt{2}}(|000\rangle + |111\rangle)$ [49], although the subsystems do not present quantum correlation, the entire system may still contain some kind of quantum correlations. Based on this consideration, we will try to capture the multipartite correlations in the entire Kitaev chains with global nonlocality, i.e., $\mathcal{S} = \mathcal{S}(\hat{\rho}_T)$.

Figure 10(a) illustrates global nonlocality in the N-size Kitaev chains at a fixed temperature $T = 0.01$. We take the curve of $N = 12$ for instance. One can see that the global nonlocality measure $\mathcal{S}$ is zero when the coupling ratio γ is small enough, and is larger than 1 when γ is large enough. Thereby, nonlocality is observed in the large-γ regions. Moreover, in the vicinity of $\gamma_0 = 0.58$, the nonlocality measure $\mathcal{S}$ undergoes a sharp transition, and its first-order derivative $\frac{d\mathcal{S}}{d\gamma}$ achieves a maximum. For large N, a scaling analysis of the transition point γ_0 is illustrated in Fig. 10(b). One can see that as N increases, γ_0 moves towards $\gamma_c = 1$ gradually, i.e., $\lim_{N \to \infty} \gamma_0 = \gamma_c$. Furthermore, at the transition point γ_0, we have also carried out a scaling analysis for the first-order derivative of $\mathcal{S}$. Please see Fig. 10(c). It is clear that, as N increases, $\frac{d\mathcal{S}}{d\gamma}|_{\gamma=\gamma_0}$ increases steadily. It indicates that $\frac{d\mathcal{S}}{d\gamma}|_{\gamma=\gamma_0}$ would diverge in the large-N limit. Finally, we conclude that the ground state of the infinite-size Kitaev chain would undergo a dramatic transition from a phase without quantum nonlocality (since $\mathcal{S} = 0$) to a phase containing quantum nonlocality (since $\mathcal{S} > 1$) at the critical point $\gamma_c = 1$. In Ref. [32], by using the string order parameter, the authors show that the QPT in the Kitaev chain has a topological nature. Our results in Fig. 10 reveal that this topological QPT is
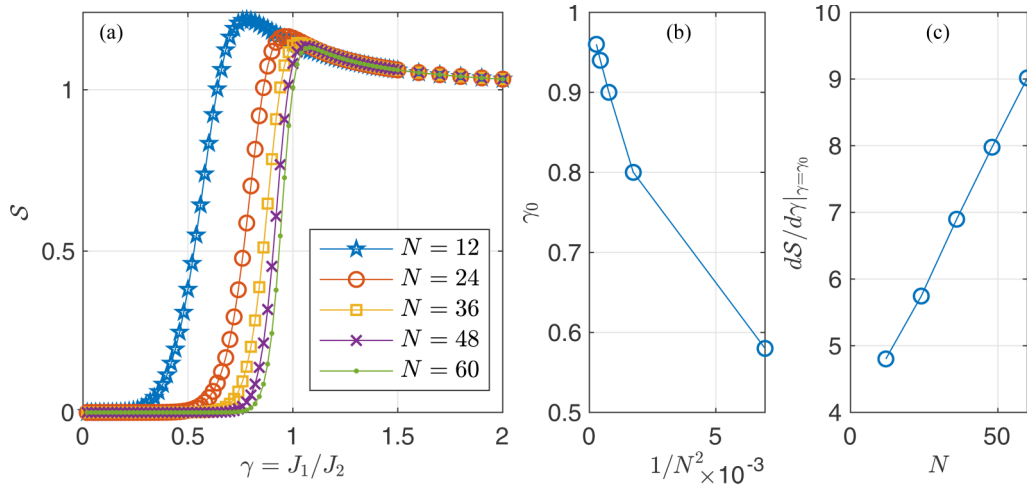
FIG. 10. (a) Global-nonlocality measure $\mathcal{S}$ in finite-size Kitaev chains as a function of the coupling ratio $\gamma = J_1/J_2$ at a fixed temperature $T = 0.01$. N denotes the total length of the chains. For finite N, the first-order derivative of $\mathcal{S}$ presents a peak point at some finite γ_0. (b) and (c) denote scaling analysis of the peak location γ_0 and the peak value $\frac{d\mathcal{S}}{d\gamma}|_{\gamma=\gamma_0}$, respectively. The results indicates that in the limit $N \to \infty$, at $\gamma_c = 1$ the ground states of the Kitaev chain would undergo a sharp transition from a phase without quantum nonlocality (since $\mathcal{S} = 0$) to a phase containing quantum nonlocality (since $\mathcal{S} > 1$).

accompanied by fundamental changes of multipartite quantum correlations.

IV. SUMMARY AND DISCUSSIONS

Multipartite nonlocality is a measure of multipartite correlations. Previous works on nonlocality in quantum chains mainly considered zero temperature. In this paper, we have extended the studies to finite temperatures.

To proceed, we have proposed a tensor-network algorithm to calculate finite-temperature nonlocality in general 1D quantum chains. We have shown that a general full-correlation Bell operator can be expressed as an MPO. Especially, the Mermin-Klyshko operator $\hat{M}$ can be exactly expressed as an MPO with a quite small bond dimension $D = 2$. With the help of this expression, the average value for $\hat{M}$ is simplified into standard 1D tensor networks (Fig. 3), which can be contracted conveniently by various software such as ITENSOR [43].

With this powerful algorithm, we have studied quantum nonlocality in three 1D spin models, i.e., the XX model, the XXZ model, and the Kitaev chain. We have mainly considered subchain nonlocality defined on the reduced density matrices of continuous n-site subchains in infinite-size systems. In order to characterize the topological QPT in the Kitaev chains, we have also investigated the global nonlocality in the entire system by considering finite-size chains.

Our first main observation is that both in the XX model and in the XXZ model, in a finite-temperature region, the logarithm nonlocality measure $\log_2 \mathcal{S}$ presents a linear decrement as the temperature rises. Details can be found in Figs. 6(b) and 7(b). It is well known that in the high-temperature limit $T \to \infty$, nonlocality should vanish. On the other hand, in the low-temperature limit $T \to 0$, one expects that the behavior of nonlocality would be determined mainly by the lowest-lying energy levels. Nevertheless, in the middle-temperature regions, our knowledge about nonlocality is still not complete. The linear behavior reported in this paper supplements

part of the missing picture in the middle-temperature regions (Fig. 11). Moreover, this linear decrement can be used to estimate precisely the threshold temperature at which multipartite nonlocality vanishes (i.e., $\log_2 \mathcal{S} = 0$).

Our second observation is that at low temperatures, the nonlocality measure can still offer us some nontrivial information about QPTs in the models.

The XX model has a second-order QPT at the critical magnetic field $h_c = 2$. We find that in the two phases the nonlocality presents quite different behavior. In the phase $h > h_c$, it holds that $\mathcal{S} \leqslant 1$ and thus nonlocality is not observed. In the phase $h < h_c$, the value of $\mathcal{S}$ is relatively large and presents an oscillation. Moreover, as the temperature rises, the oscillation survives in a finite-temperature zone. The oscillation of the nonlocality discloses that, behind the monotonic increasing magnetization curve of the model (Fig. 5), there is a hidden and rich change of multipartite correlations in the reduced density matrices $\hat{\rho}_n$ of the subchains.

For the XXZ model, we find that the nonlocality measure $\mathcal{S}$ presents a cusplike singularity at infinite-order QPT point $\Delta_c = 1$ even at finite temperatures.

Nevertheless, the most interesting result in this paper may be about the Kitaev chain. The ground states of the Kitaev chain are degenerate for any finite γ, and undergo a topological-type QPT at the critical point $\gamma_c = 1$. We have used the thermal-state operator $e^{-\beta\hat{H}}$ to capture all the degen-
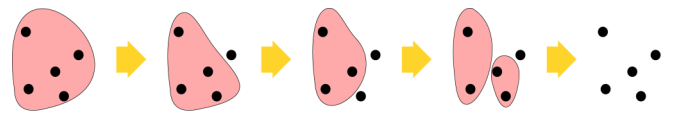
FIG. 11. The linear behavior $\log_2 \mathcal{S} \approx -aT + b$ reveals an intuitive picture about how thermodynamic fluctuations *melt* multipartite nonlocality in quantum systems. (At least) in the vicinity of the threshold value $\log_2 \mathcal{S} = 0$, as the temperature T rises the hierarchy of multipartite nonlocality decreases steadily and linearly.

erate ground states of the models. Numerical results indicate that in the limit $T \to 0$ and $n \to \infty$, the subchain nonlocality measure $\mathcal{S}$ would be zero for $\gamma < 1$, and be nonzero for $\gamma > 1$ (Fig. 9). Thereby, $\mathcal{S}$ may be regarded as an alternative order parameter to characterize this topological QPT. Furthermore, by considered global nonlocality in finite-size Kitaev chains (Fig. 10), we find that in the limit $N \to \infty$, at $\gamma_c = 1$ the system would undergo a *dramatic* transition from a phase without nonlocality (since $\mathcal{S} = 0$) to a phase containing nonlocality (since $\mathcal{S} > 1$). The mechanism for multipartite nonlocality to successfully capture this QPT is that, just as the string-order operators $\hat{\Delta}_{x,y}$ used in Ref. [32], the Mermin-Klyshko operator $\hat{M}_{[1...n]}$ is also a long-range operator. Their difference is that the construction of $\hat{\Delta}_{x,y}$ depends upon an analytical understanding of the *specific* models, and the construction of $\hat{M}_{[1...n]}$ does not depend upon *a priori* knowledge of the models. Instead, it relies on a *general* numerical optimization [Eq. (5)]. It would be interesting to check the behavior of multipartite nonlocality in similar quantum models which undergo topological-type QPTs, such as the bond-alternating spin-1/2 Heisenberg chains [50].

Finally, we would like to provide some comments on the MPO form of the Bell operators. This presentation may disclose some insight to our previous numerical results in both 1D quantum chains [26,28] and 2D quantum lattices [29]. It is well known that the Mermin-Klyshko inequality is closely related to a typical genuine multipartite entangled state, i.e., the GHZ state $|\psi_{\text{GHZ}}\rangle = \frac{1}{\sqrt{2}}(|00 \cdots 0\rangle + |11 \cdots 1\rangle)$. Explicitly, the Mermin-Klyshko inequality $\mathcal{S} \leqslant 1$ is maximally violated by the GHZ state with $\mathcal{S}(|\psi_{\text{GHZ}}\rangle) = 2^{\frac{n-1}{2}}$. When we use the Mermin-Klyshko operator to characterize several 1D quantum chains, the nonlocality measure $\mathcal{S}$ is found to scale as $\mathcal{S} \sim 2^{an}$ with $a \leqslant \frac{1}{2}$ a model-dependent constant [26,28]. Thus we believe the Mermin-Klyshko operator has successfully captured part of the features of multipartite correlations in these chains. Its success has some underlying mechanism. From Eq. (18) one can see that the coefficient tensor B_i of the Mermin-Klyshko operator is *translation invariant* (except for the two boundary points). Thus there is some hidden adaption or matching between our tool (the Mermin-Klyshko operator) and our research objects (these translation-invariant 1D quantum chains). An interesting question is whether the Mermin-Klyshko operator would be a good Bell operator to characterize 2D quantum states. It is clear that we can always transform a given 2D tensor network state into an MPS [29]. Nevertheless, this MPS is *physically* not translation invariant any more. Thereby, when the Mermin-Klyshko operator is used to characterize this MPS, some hidden mismatch would occur. Based on this consideration, we argue that the Mermin-Klyshko operator may not be the best Bell operator to analyze 2D quantum states.

It needs mention that even if just translation-invariant quantum states are considered the Mermin-Klyshko inequality may still not be an *optimal* Bell inequality to exhibit the strongest violation. In fact, the violation of the Mermin-Klyshko inequality is a sufficient but not a necessary condition to detect general multipartite correlations. A well-known example is another typical genuine multipartite entangled state—the W state $|\psi_W\rangle = \frac{1}{\sqrt{3}}(|001\rangle + |010\rangle + |100\rangle)$ [51]. The Mermin-Klyshko inequality is just slightly violated by the W state [13]. Instead, some special Bell inequalities have been constructed so as to exhibit strong violation [16]. Nevertheless, the construction of these special Bell inequalities depends heavily upon *a priori* knowledge of the W state, thus the approach seems to be useless for us to construct *optimal* Bell inequalities for other general quantum states.

We argue that the MPO representation of the general full-correlation Bell operator, i.e., $\hat{M}_g(\beta_{k_1 k_2 \dots k_n}) = \hat{M}_g(B_1^{k_1}, B_2^{k_2}, \cdots B_n^{k_n})$, may offer an alternative approach for us to numerically construct *optimal* Bell inequalities for general 1D quantum lattices. The goal is to figure out optimal coefficient tensors $\{B_i\}$ for some given $\hat{\rho}_n$, so as to exhibit strong violation. As in the Mermin-Klyshko operator, it would be quite reasonable to just consider translation-invariant coefficient tensors B_i, i.e., $B_i = \tilde{B}$ for $1 < i < n$, with $\tilde{B}$ a $2 \times D \times D$ tensor. Thereby, the general Bell operator $\hat{M}_g(\beta_{k_1 k_2 \dots k_n})$, which seems to depend upon 2^n parameters, turns out to be $\hat{M}_g(\tilde{B})$ with merely $2D^2$ free parameters. It is much easier to optimize $\hat{M}_g$ with respect to these $2D^2$ parameters, rather than 2^n parameters, to figure out an optimal Bell inequality. Whether or not this idea is practical would be checked in our future research.

[1] R. Horodecki, P. Horodecki, M. Horodecki, and K. Horodecki, Rev. Mod. Phys. **81**, 865 (2009).

[2] G. F. A. Osterloh, L. Amico, and R. Fazio, Nature (London) **416**, 608 (2002).

[3] G. Vidal, J. I. Latorre, E. Rico, and A. Kitaev, Phys. Rev. Lett. **90**, 227902 (2003).

[4] L.-A. Wu, M. S. Sarandy, and D. A. Lidar, Phys. Rev. Lett. **93**, 250404 (2004).

[5] O. Legeza and J. Sólyom, Phys. Rev. Lett. **96**, 116401 (2006).

[6] W. K. Wootters, Phys. Rev. Lett. **80**, 2245 (1998).

[7] J. Eisert, M. Cramer, and M. B. Plenio, Rev. Mod. Phys. **82**, 277 (2010).

[8] S. Sachdev, *Quantum Phase Transitions* (Cambridge University, Cambridge, England, 1999).

[9] O. Gühne, G. Tóth, and H. J. Briegel, New J. Phys. **7**, 229 (2005).

[10] F. Levi and F. Mintert, Phys. Rev. Lett. **110**, 150402 (2013).

[11] D. Collins, N. Gisin, S. Popescu, D. Roberts, and V. Scarani, Phys. Rev. Lett. **88**, 170405 (2002).

[12] Q. Y. He, E. G. Cavalcanti, M. D. Reid, and P. D. Drummond, Phys. Rev. Lett. **103**, 180402 (2009).

[13] J.-D. Bancal, C. Branciard, N. Gisin, and S. Pironio, Phys. Rev. Lett. **103**, 090503 (2009).

[14] J. Batle and M. Casas, J. Phys. A: Math. Theor. **44**, 445304 (2011).

[15] J.-D. Bancal, N. Brunner, N. Gisin, and Y.-C. Liang, Phys. Rev. Lett. **106**, 020405 (2011).

[16] N. Brunner, J. Sharam, and T. Vértesi, Phys. Rev. Lett. **108**, 110501 (2012).

[17] X. Wang, C. Zhang, Q. Chen, S. Yu, H. Yuan, and C. H. Oh, Phys. Rev. A **94**, 022110 (2016).

[18] J. Bowles, J. Francfort, M. Fillettaz, F. Hirsch, and N. Brunner, Phys. Rev. Lett. **116**, 130401 (2016).

[19] J.-D. Bancal, J. Barrett, N. Gisin, and S. Pironio, Phys. Rev. A **88**, 014102 (2013).

[20] G.-B. Xu, Q.-Y. Wen, S.-J. Qin, Y.-H. Yang, and F. Gao, Phys. Rev. A **93**, 032341 (2016).

[21] S. Campbell and M. Paternostro, Phys. Rev. A **82**, 042324 (2010).

[22] L. Justino and T. R. de Oliveira, Phys. Rev. A **85**, 052128 (2012).

[23] D.-L. Deng, C. Wu, J.-L. Chen, S.-J. Gu, S. Yu, and C. H. Oh, Phys. Rev. A **86**, 032305 (2012).

[24] Z.-Y. Sun, Y.-Y. Wu, J. Xu, H.-L. Huang, B.-F. Zhan, B. Wang, and C.-B. Duan, Phys. Rev. A **89**, 022101 (2014).

[25] Z.-Y. Sun, S. Liu, H.-L. Huang, D. Zhang, Y.-Y. Wu, J. Xu, B.-F. Zhan, H.-G. Cheng, C.-B. Duan, and B. Wang, Phys. Rev. A **90**, 062129 (2014).

[26] Z.-Y. Sun, B. Guo, and H.-L. Huang, Phys. Rev. A **92**, 022120 (2015).

[27] Y. Dai, C. Zhang, W. You, Y. Dong, and C. H. Oh, Phys. Rev. A **96**, 012336 (2017).

[28] H.-G. Cheng, M. Li, Y.-Y. Wu, M. Wang, D. Zhang, J. Bao, B. Guo, and Z.-Y. Sun, Phys. Rev. A **101**, 052116 (2020).

[29] Z.-Y. Sun, X. Guo, and M. Wang, Eur. Phys. J. B **92**, 75 (2019).

[30] J. Bao, B. Guo, H.-G. Cheng, M. Zhou, J. Fu, Y.-C. Deng, and Z.-Y. Sun, Phys. Rev. A **101**, 012110 (2020).

[31] Z.-Y. Sun, M. Wang, Y.-Y. Wu, and B. Guo, Phys. Rev. A **99**, 042323 (2019).

[32] X.-Y. Feng, G.-M. Zhang, and T. Xiang, Phys. Rev. Lett. **98**, 087204 (2007).

[33] X.-G. Wen, Int. Scholar. Res. Notices **2013**, 198710 (2013).

[34] N. D. Mermin, Phys. Rev. Lett. **65**, 1838 (1990); G. Svetlichny, Phys. Rev. D. **35**, 3066 (1987).

[35] A. V. Belinskiî and D. N. Klyshko, Phys. Usp. **36**, 653 (1993).

[36] V. Scarani and N. Gisin, J. Phys. A: Math. Gen. **34**, 6043 (2001).

[37] R. Orús, Ann. Phys. (NY) **349**, 117 (2014).

[38] R. F. Werner and M. M. Wolf, Phys. Rev. A **64**, 032112 (2001).

[39] U. Schollwöck, Ann. Phys. (NY) Special Issue **326**, 96 (2011).

[40] B. Pirvu, V. Murg, J. I. Cirac, and F. Verstraete, New J. Phys. **12**, 025012 (2010).

[41] F. Verstraete, J. J. García-Ripoll, and J. I. Cirac, Phys. Rev. Lett. **93**, 207204 (2004).

[42] D. E. Parker, X. Cao, and M. P. Zaletel, Phys. Rev. B **102**, 035147 (2020).

[43] M. Fishman, S. R. White, and E. M. Stoudenmire, arXiv:2007.14822.

[44] B. Bauer, L. D. Carr, H. G. Evertz, A. Feiguin, J. Freire, S. Fuchs, L. Gamper, J. Gukelberger, E. Gull, S. Guertler, A. Hehn, R. Igarashi, S. V. Isakov, D. Koop, P. N. Ma, P. Mates, H. Matsuo, O. Parcollet, G. Pawłowski, J. D. Picon *et al.*, J. Stat. Mech.: Theory Exp. (2011) P05001.

[45] J. Vidal, G. Palacios, and C. Aslangul, Phys. Rev. A **70**, 062304 (2004).

[46] J. I. Latorre, R. Orús, E. Rico, and J. Vidal, Phys. Rev. A **71**, 064101 (2005).

[47] A. Kitaev, Ann. Phys. (NY) Special Issue **321**, 2 (2006).

[48] H.-D. Chen and Z. Nussinov, J. Phys. A: Math. Theor. **41**, 075001 (2008).

[49] A. Z. D. M. Greenberger, M.A. Horne, *Bell's Theorem, Quantum Theory, and Conceptions of the Universe* (Academic, New York, 1989).

[50] H. T. Wang, B. Li, and S. Y. Cho, Phys. Rev. B **87**, 054402 (2013).

[51] W. Dür, G. Vidal, and J. I. Cirac, Phys. Rev. A **62**, 062314 (2000).